UNCLASSIFIED

AD NUMBER

AD272834

NEW LIMITATION CHANGE

TO

Approved for public release, distribution unlimited

FROM

Distribution authorized to U.S. Gov't. agencies and their contractors; Administrative/Operational Use; MAR 1962. Other requests shall be referred to Arnold Engineering Development Center, Arnold AFS, TN.

AUTHORITY

AFFDL ltr, 21 Oct 1974

THIS PAGE IS UNCLASSIFIED

UNCLASSIFIED

AD 272 834

Reproduced
by the

ARMED SERVICES TECHNICAL INFORMATION AGENCY
ARLINGTON HALL STATION
ARLINGTON 12, VIRGINIA

UNCLASSIFIED

Best Available Copy

NOTICE: When government or other drawings, specifications or other data are used for any purpose other than in connection with a definitely related government procurement operation, the U. S. Government thereby incurs no responsibility, nor any obligation whatsoever; and the fact that the Government may have formulated, furnished, or in any way supplied the said drawings, specifications, or other data is not to be regarded by implication or otherwise as in any manner licensing the holder or any other person or corporation, or conveying any rights or permission to manufacture, use or sell any patented invention that may in any way be related thereto.

AEDC-TDR-62-39

272 834

CATALOGUED BY ASTIA AS AD NO.

PRESSURE DISTRIBUTION, HEAT TRANSFER, AND DRAG TESTS ON THE GOODYEAR BALLUTE AT MACH 10

By

L. D. Kayser
von Kármán Gas Dynamics Facility

ARO, Inc.

TECHNICAL DOCUMENTARY REPORT NO. AEDC-TDR-62-39

March 1962

AFSC Program Area 720F, Project 6065, Task 61256

(Prepared under Contract No. AF 40(600)-800 S/A 24(61-73) by ARO, Inc., contract operator of AEDC, Arnold Air Force Station, Tennessee)

$3.00

ARNOLD ENGINEERING DEVELOPMENT CENTER
AIR FORCE SYSTEMS COMMAND
UNITED STATES AIR FORCE

NO OTS

PRESSURE DISTRIBUTION, HEAT TRANSFER, AND DRAG TESTS ON THE GOODYEAR BALLUTE AT MACH 10

By

L. D. Kayser
von Kármán Gas Dynamics Facility
ARO, Inc.
a subsidiary of Sverdrup and Parcel, Inc.

March 1962

ARO Project No. 351217

ABSTRACT

Heat transfer and pressure distribution tests were conducted on rigid models of the ballute, and drag measurements were obtained on flexible models which were either inflated with ram air or pre-inflated with a bladder. The flexible models were fabricated from a woven stainless-steel cloth (René 41 cloth) and impregnated with a silicone polymer to decrease porosity. The Reynolds number range investigated was from 0.36×10^6 to 1.80×10^6 per foot, and all data were obtained at zero angle of attack.

CONTENTS

ILLUSTRATIONS

NOMENCLATURE

b	Model skin thickness, ft
C_D	Drag coefficient, drag/q_∞ S
C_p	Pressure coefficient, $p - p_\infty/q_\infty$
c	Specific heat of model material, Btu/lb_m - °R
D	Diameter of the Ballute at the equator, D = 10 in.
d	Diameter of forebody, in.
h	Heat transfer coefficient based on temperatures, Btu/sec - ft^2 - °R
h_i	Heat transfer coefficient based on enthalpies, lb_m/ft^2 - sec
i	Enthalpy of air, Btu/lb_m
ℓ	Distance between base of forebody and nose of the Ballute, in.
p	Local pressure, psia
Q	Heat transfer rate, Btu/ft^2 - sec
q	Dynamic pressure, psia
Re	Reynolds number
S	Reference area, 78.5 $in.^2$
s	Curvilinear surface distance in the longitudinal direction, in. (s = 0 at the equator)
T	Temperature, °R
t	Time, sec
w	Specific weight of model material, lb_m/ft^2

SUBSCRIPTS

o	Stagnation conditions
w	Conditions at model wall
∞	Tunnel free-stream conditions

1.0 INTRODUCTION

At the request of the Aeronautical Systems Division, Air Force Systems Command (AFSC), pressure distribution, heat transfer, and drag tests on scale models of the Ballute were conducted for Goodyear Aircraft Corporation at a nominal Mach number of 10 and free-stream unit Reynolds numbers from 0.36×10^6 to 1.80×10^6 per foot. The tests were performed in the 50-Inch Mach 10 Tunnel of the von Kármán Gas Dynamics Facility (VKF), Arnold Engineering Development Center, AFSC, during the periods of November 9-11, 1961, November 16, 1961, and November 28, 1961. All data were obtained with the model at zero angle of attack.

Spark shadowgraphs and shadowgraph movies were obtained during the pressure model runs. High-speed movies of the flexible models were obtained during the drag runs.

2.0 APPARATUS

2.1 WIND TUNNEL

The 50-Inch Mach 10 Tunnel is an axisymmetric, continuous-flow, variable-density, hypersonic wind tunnel with a 50-in.-diam test section. Because of changes in boundary-layer thickness caused by changing pressure level, the Mach 10 contoured nozzle produces an average test section Mach number which varies from 10.0 at a stagnation pressure of 200 psia to 10.2 at 2000 psia. The centerline flow distribution is uniform within about 0.5 percent in Mach number. There is a slight axial gradient on the order of 0.01 Mach number per foot.

Details of the 50-Inch Mach 10 Tunnel and associated equipment are shown in Fig. 1. The hydraulically driven, angle-of-attack mechanism pitches the model in a vertical plane from -15 to 15 deg. The remotely controlled, water-cooled, roll mechanism is electrically driven and is capable of rotating the model-sting combination ±180 deg.

A unique feature of the 50-Inch Mach 10 Tunnel is the model installation chamber below the test section which allows the entire pitch mechanism, sting, and model to be lowered out of the tunnel. When the

---

Manuscript released by author January 1962.

model is in the retracted position the fairing doors and the safety doors can be closed (Fig. 1), allowing entrance to the tank for model changes while the tunnel is running. When the model is in the test section, only the fairing doors are closed, leaving the tank at tunnel static pressure.

Stagnation pressures up to approximately 2000 psia are supplied to the 50-Inch Mach 10 Tunnel by the VKF Compressor Plant. The air is selectively valved through the compressor plant, the high-pressure driers, and the propane-fired heater, which raises the air temperature to a maximum of 800°F. The heated air then enters the electric heater which increases the air temperature to a maximum of 1450°F, sufficient to prevent liquefaction of the air in the test section. From the electric heater, the air flows through the nozzle, the diffuser, the cooler, and back into the compressor system.

2.2 MODELS AND SUPPORT

The basic external geometry for all Ballute models is shown in Fig. 2.

The heat transfer model was fabricated from 321 stainless steel and was formed by the spinning process. The skin thickness varied from 0.050 to 0.064 in. Nineteen thermocouples were spot-welded on the interior surface and were located as shown in Fig. 2. Two thermocouples were also mounted inside the model to measure the internal ambient temperature.

The pressure model was fabricated from 321 stainless steel and was instrumented with 17 static orifices on the surface (Fig. 2) and one internal orifice for measuring the internal model pressure.

Flexible drag models were fabricated from René 41 cloth, which is woven from stainless-steel fibre. The seams of the model were joined by spot welding, and the model was impregnated with a high temperature silicone polymer to decrease the porosity. For added strength, eight longitudinal cables were connected from the nozzle to the base plate. A partially inflated Ballute is shown in Fig. 3.

The basic inlet configuration is shown in Fig. 4. This inlet was tested on the pressure model with screens covering the inlet slots, with reed valves (screen removed), and with open slots. In addition to the basic inlet, two types of total head inflating probes were used with the flexible models (Figs. 5c-d).

The models were supported by the strut assembly as shown in Figs. 6 and 7. The leading edges of the vertical sections and the sides and top of the horizontal section were water-cooled. The flexible drag models were connected to a 3/32-in.-diam René cable which was routed around pulley wheels inside the strut. The cable could be extended or retracted by means of a hydraulic cylinder which was mounted in the bottom portion of the strut. The pressure and heat transfer models were supported with a 1.75-in.-diam sting, as shown in Fig. 7; also, by means of a collet-type sting, which replaces the hemispherical cover, the sting length of the heat transfer and pressure models could be adjusted as desired. Figures 8 and 9 are installation photographs of the pressure model.

2.3 INSTRUMENTATION

Pressure

The pressure data system consists basically of nine channels, each of which is time-shared between eleven model orifices by means of 12-position Giannini pressure switching valves. The total capability is 99 model measurements, with the first position of each pressure switching valve being used for transducer calibration.

Each channel includes two pressure measuring transducers (referenced to hard vacuum). The two measuring transducers, a ±1 psid unit and a 0-15 psid unit, are switched in and out of the system automatically to allow measuring to the best available precision. If the sensed pressure level is above 15 psia, the reference side of the 15-psid transducer is vented to atmosphere to extend the measuring range.

The measuring system is of the Wiancko frequency modulation type. Precision frequency modulation oscillators, frequency multipliers, binary counters, and a time base generator operate in conjunction with the transducers to obtain a differential count of 10,000. The resulting resolution is 0.0002 psi for the 1-psi transducer and 0.0015 psi for the 15-psid transducers. The accumulated count is stored in the binary counters, read out serially by the ERA scanner, and punched on paper tape.

The p_o system contains two channels of frequency modulation pressure instrumentation, one with a range of 0-500 psia and the other with a range of 0-2500 psia.

Heat Transfer Phase

The reference junction of each thermocouple was maintained at 132°F. Each thermocouple output was recorded in digital form on magnetic tape at a rate of 20 times per second by means of a Beckman 210 analog-to-digital converter. To monitor the temperatures at selected points on the models, nine of the thermocouple outputs were also recorded on strip charts by 0.25-second (full-scale travel) Brown servopotentiometers.

General

The tunnel stagnation pressure and temperature were measured in the stilling chamber. A 2500-psid transducer, referenced to vacuum, and a chromel-alumel thermocouple were used for the measurement. A conventional, short-range, divergent-ray, spark shadowgraph system was used to record selected flow patterns about the model.

Drag Phase

A strain-gage drag link furnished by Goodyear Aircraft was used for drag measurements on the flexible models. The drag link was instrumented with two strain-gage bridges and mounted on the hydraulic cylinder piston rod. Power to the strain-gage bridges was supplied from a 400-cps carrier system. Output from one of the bridges was measured with a null-balance servopotentiometer with a shaft positioning digitizer for recording on punched paper tape; the other strain-gage output was measured with a galvanometer-type oscillograph (visicorder).

A cable positioning potentiometer was also mounted inside the strut assembly. Output from this potentiometer was also measured with the servopotentiometer and visicorder.

3.0 TEST DESCRIPTION

3.1 TEST PROCEDURE

Pressure data were obtained at various distances behind the forebody, and heat transfer data were obtained at an ℓ/d of 18. All data were obtained at zero-deg angle of attack, and the Reynolds number range covered was from 0.36×10^6 to 1.80×10^6 per foot. The forebody and strut assembly were removed, and additional heat transfer and pressure data were obtained over the same Reynolds number range.

The flexible models were installed, as shown in Fig. 6, and injected into the tunnel at the minimum desired ℓ/d. The cable was then extended, and drag measurements were obtained over the desired ℓ/d range. Some of the flexible models were pre-inflated with a neoprene bladder (Figs. 5a and b); other models were inflated with the ram air devices shown in Figs. 5c and d. In order to keep the models relatively stable during the injection, a restraining cable was loosely connected from the model base to the hemispherical cover.

3.2 DATA REDUCTION PROCEDURE

The strain-gage and cable positioning potentiometer sensitivities were obtained from a static calibration. From these sensitivities, the model drag and position (ℓ) were computed. A drag coefficient was computed using the maximum cross-sectional area of the model (78.5 in.^{2}).

Pressure transducer sensitivities obtained by a dead-weight calibration were used in the data reduction program for computation of pressures. The parameters of C_p, p/p_∞, and p/p_o were computed for each pressure.

The heat transfer rates were computed using the equation $Q = wbc\,(dT_w/dt)$. The slope dT_w/dt was calculated by taking the first derivative of a least squares parabola which was fitted to 21 data points taken at 0.05-second intervals. Slopes were obtained at times of 0.2, 0.5, 1.0, 2.0, and 5.0 seconds from the time the model reached the tunnel centerline. A complete set of data was computed for each of the five times. One heat transfer coefficient was computed using temperatures $h = Q/T_o - T_w$ and another was computed using enthalpies $h_i = Q/\,i_o - i_w$. The enthalpies were obtained from the tabulated values of Ref. 1.

Tunnel free-stream conditions were computed assuming isentropic expansion of a Beattie-Bridgeman gas with variable specific heats. Empirical equations of the form

$$\frac{p_\infty/p_o}{(p_\infty/p_o)_{ideal}} = f(p_o,\ T_o) \text{ and } \frac{T_\infty/T_o}{(T_\infty/T_o)_{ideal}} = f(p_o,\ T_o)$$

were obtained from calculations based on the Beattie-Bridgeman equation of state (Ref. 2). The ideal ratios in the denominator of the above equations were computed from the perfect gas relations of Ref. 3. The correction values, $f(p_o,\ T_o)$, ranged from 0.96 to 1.05.

4.0 RESULTS AND DISCUSSION

The original test objective was to obtain pressure and heat transfer data on rigid models of the Ballute mounted aft of the forebody with a connecting riser line. The flexible models were to have been packed inside a three-in. -diam cannister (Fig. 9), deployed into the airstream, and inflated by ram air through the basic inlet. The ℓ/d range to be investigated was from 4 to 10. Because pressure distributions indicated that the flexible models would not inflate properly, the test was not conducted according to the original plan.

Figure 10 shows the pressure distribution for various Reynolds numbers at an ℓ/d of 18. At the lowest Reynolds number the pressure ratios on the front surface were lower than at the higher Reynolds numbers. Several groups of data were obtained with open inlet at Reynolds numbers of 1.80×10^6 per foot and ℓ/d values ranging from 7-18. The pressure distribution for these groups was essentially the same as the plugged inlet distribution at the same Reynolds number. The internal pressure ranged from 5.5 to 9.0 times free-stream static pressure, which was insufficient to fully inflate the Ballute.

Several attempts were made to close the wake between the forebody and the model, and hence, increase the internal pressure. The following expedients were attempted without success: the ℓ/d values were increased to the maximum attainable value of 18; two rows of 0.25-in. steel balls were spot-welded on the forebody (Fig. 8); and holes were drilled around the perimeter of the cannister step (Fig. 9).

Pressures which were obtained without the forebody and strut assembly are shown in Fig. 11. The higher pressure ratios on the windward portion of the model were apparently independent of Reynolds number. The pressure ratios aft of the equator decreased slightly with increasing Reynolds number. The internal pressures which were obtained with an open inlet were essentially equal to the computed values of stagnation pressure behind a normal shock.

Figures 12 and 13 show the heat transfer coefficients which were obtained two seconds after the model reached the tunnel centerline. These coefficients represent the storage heat transfer rates only and do not include corrections for conduction or radiation losses. Some surface conduction values were computed and found to be small. Radiation terms were negligible since the model temperatures did not vary significantly from the tunnel wall temperature. Heat transfer rates on the windward portion of the model were as much as twice as high when the model was tested without the forebody.

Because of the inability to obtain high internal pressures with the basic inlet, a flexible model was pre-inflated with a neoprene bladder and injected into the tunnel at an ℓ/d of approximately 10 and a Reynolds number of 0.96×10^6. The model was completely stable, and the measured drag coefficient was 0.31. The model was withdrawn from the tunnel after approximately 25 seconds, and although the bladder was destroyed, there was no visible damage to the model.

At a later tunnel entry, the flexible drag model setup was re-installed. Two of the models were tested with the total head inflating probes shown in Figs. 5c and d, and one model without probes was again pre-inflated with a bladder (Figs. 5a and b).

The bladder inflated model was injected into the tunnel at an ℓ/d of 4. The model was slightly unstable upon injection but became stable after a slight increase in ℓ/d. The model remained in the tunnel for approximately 70 seconds before rupturing. The cause of failure appeared to be excessive internal model pressure. Drag coefficients for this run are presented in Fig. 14.

A model with the forward-mounted inflating probes (Fig. 5c) was injected into the tunnel and appeared to inflate satisfactorily. However, the model ruptured immediately and no drag data were obtained.

A model with aft-mounted inflating probes (Fig. 5d) was injected into the tunnel for a period of approximately 17 seconds and retracted before any damage occurred. The model inflated satisfactorily, and drag measurements were obtained over the ℓ/d range from 6 to 11. Coefficients for this run are presented in Fig. 15 (run 7). The same model was again injected into the tunnel at an ℓ/d of zero, but the model failed within a few seconds and no drag measurements were taken. The aft-mounted probes were installed on another model and injected into the tunnel at $\ell/d = 0$. The model inflated satisfactorily and was stable over the ℓ/d range from zero to 8.5. Drag coefficients for this run are presented in Fig. 15 (run 9). The discontinuity shown in the drag coefficients at ℓ/d of 6.5 (Fig. 15) indicates that there may be a critical value of ℓ/d. The discontinuity occurred at several points of run 9 and one point of run 7. The bladder-inflated model (Fig. 14) had an apparent discontinuity at an ℓ/d of 4 and perhaps was different from the ℓ/d value of 6.5 because of a Reynolds number effect. The discontinuity may have been caused by a separated region between the forebody and the model which disappeared as the model was moved aft. It would seem reasonable that such a separated region for the lower Reynolds number runs (Fig. 15) would occur over a larger ℓ/d range. Comparison of Figs. 14 and 15 shows that this was the case.

Drag coefficients obtained by integration of pressures (Fig. 14) on the rigid model were smaller than those obtained on the flexible drag models. The higher values of drag obtained on the flexible models may be attributed to the following reasons: The photographs of Fig. 5 show that the flexible models did not assume a shape identical to the rigid models when fully inflated; the cables, cable hold-down material, and the rougher surface of the flexible models (Fig. 3) would tend to increase the drag; since the flexible models were supported only by the longitudinal riser line, the weight of the model would induce a small angle of attack. Decreasing the Reynolds number decreased the calculated drag coefficient, except when the pressures were obtained without the presence of the forebody and strut assembly. Drag coefficients of 0.5 were obtained by pressure integration when the forebody was removed.

Figure 16 is a shadowgraph of the pressure model with plugged inlet, and Fig. 17 is a shadowgraph of the pressure model with open inlet.

REFERENCES

1. "Handbook of Supersonic Aerodynamics." NAVORD Report 1488 (Vol. 5).

2. Randall, R. E. "Thermodynamic Properties of Air: Tables and Graphs Derived from the Beattie Bridgeman Equation of State Assuming Variable Specific Heats." AEDC-TR-57-8, August 1957

3. Ames Research Staff. "Equations, Tables, and Charts for Compressible Flow." NACA Report 1135, 1953.

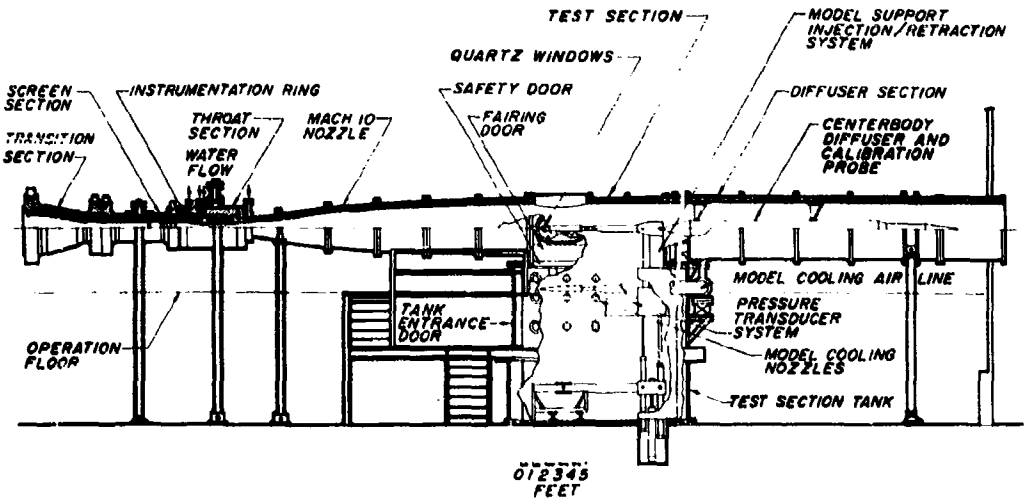

a. Tunnel Assembly

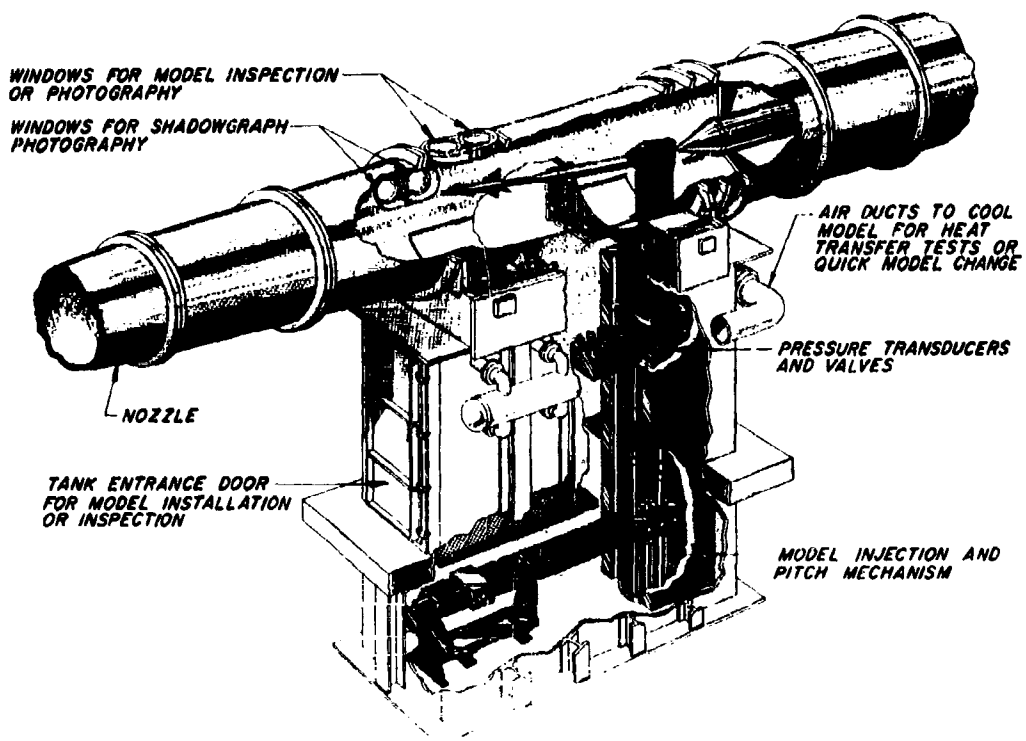

b. Tunnel Test Section

Fig. 1 Details of the 50-In. Mach 10 Tunnel

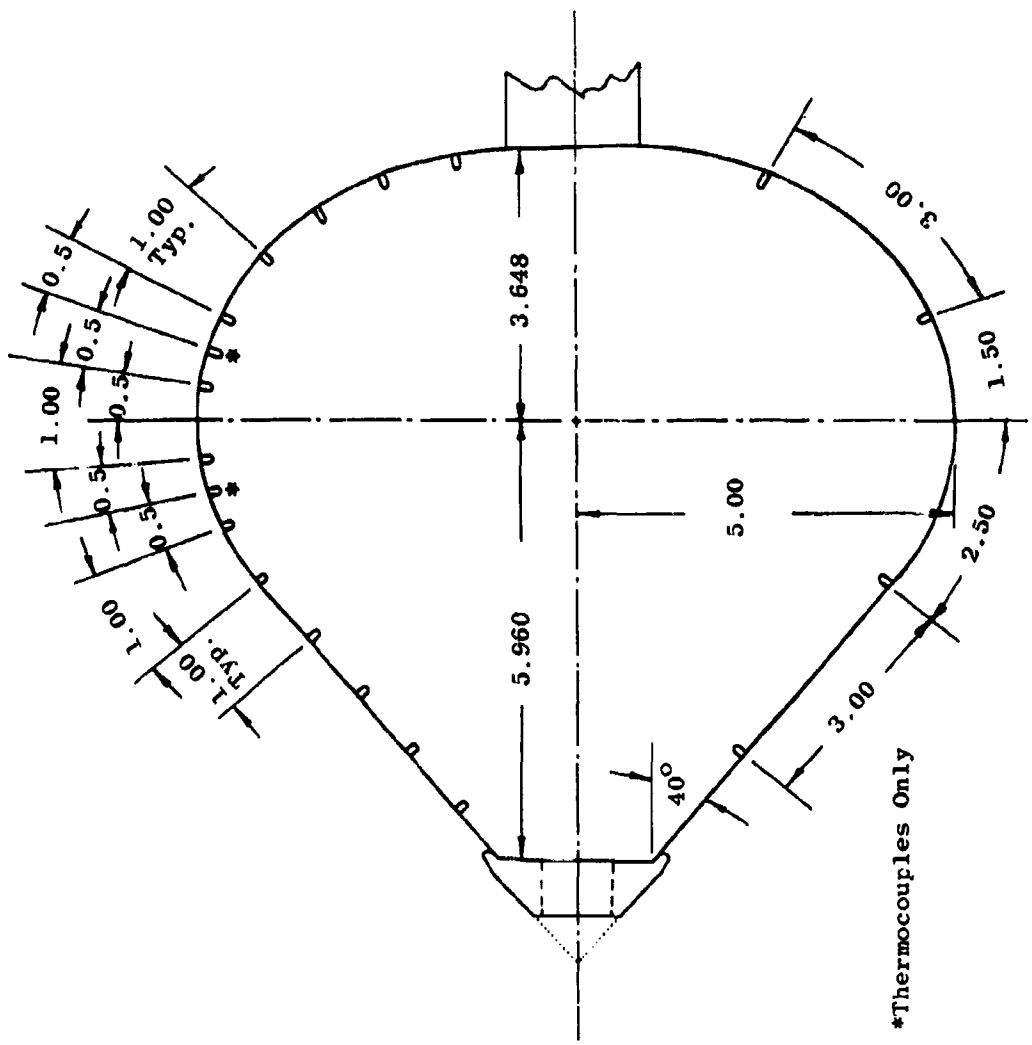

Fig. 2 Ballute Geometry, Thermocouple and Pressure Tap Locations

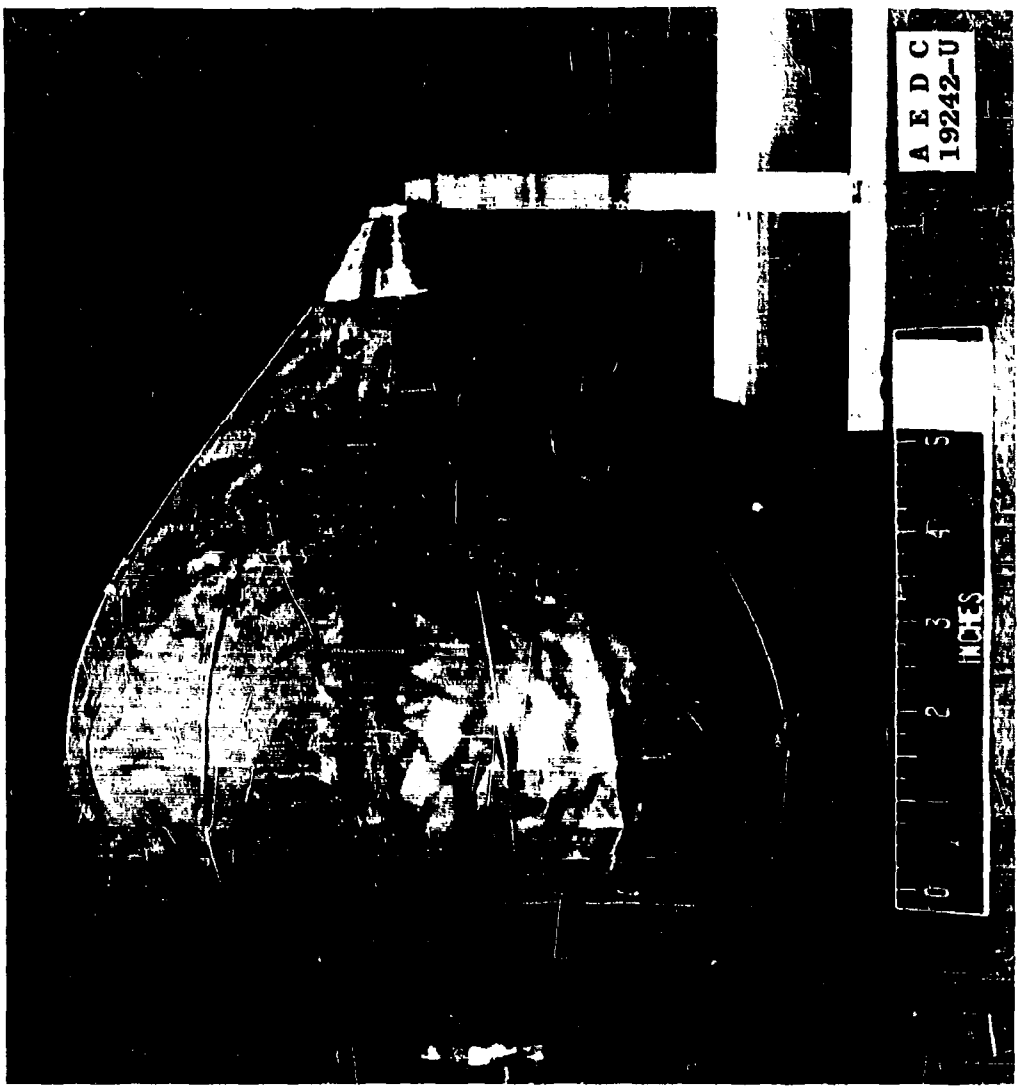

Fig. 3 Photograph of Flexible Model

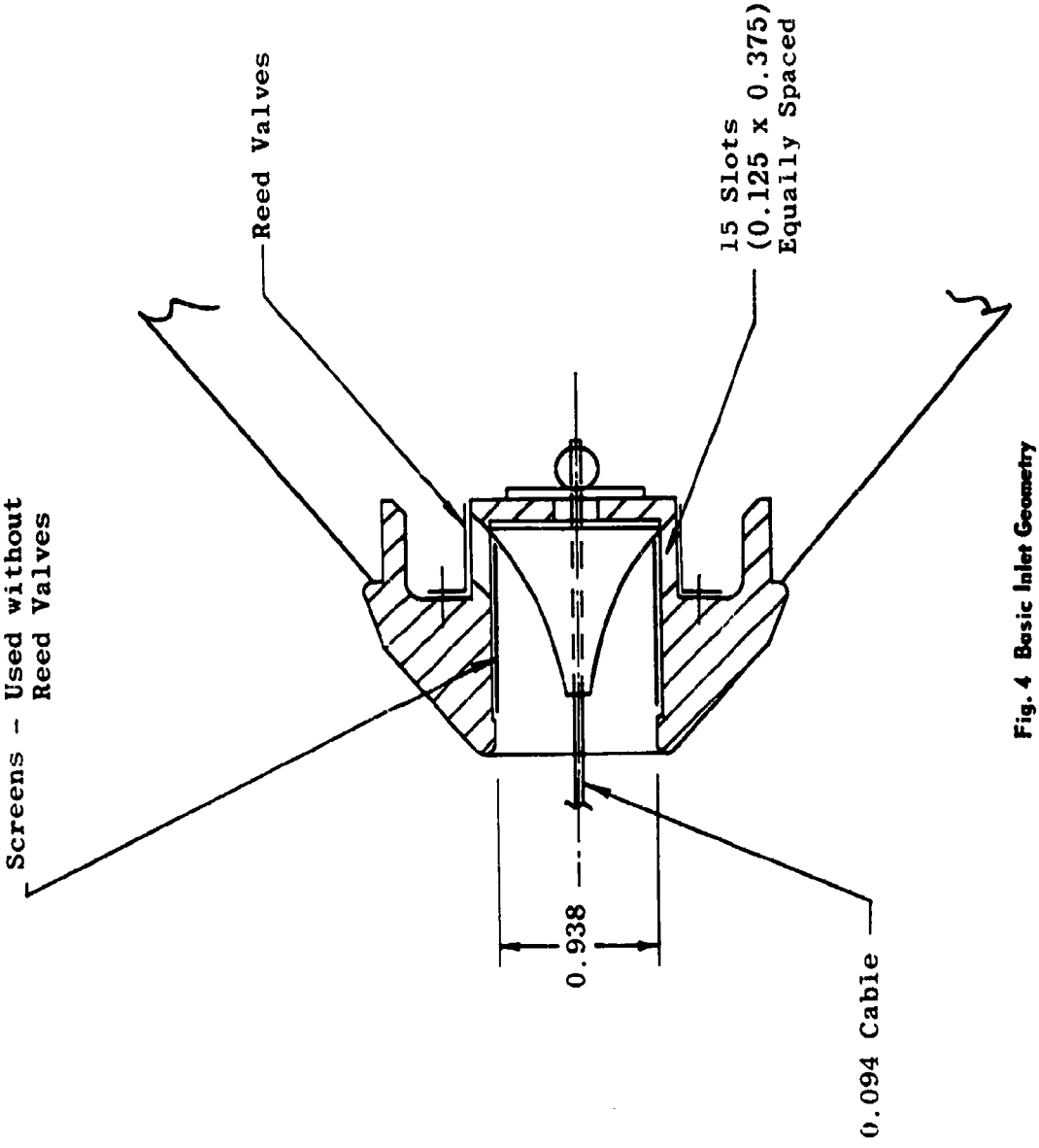

Fig. 4 Basic Inlet Geometry

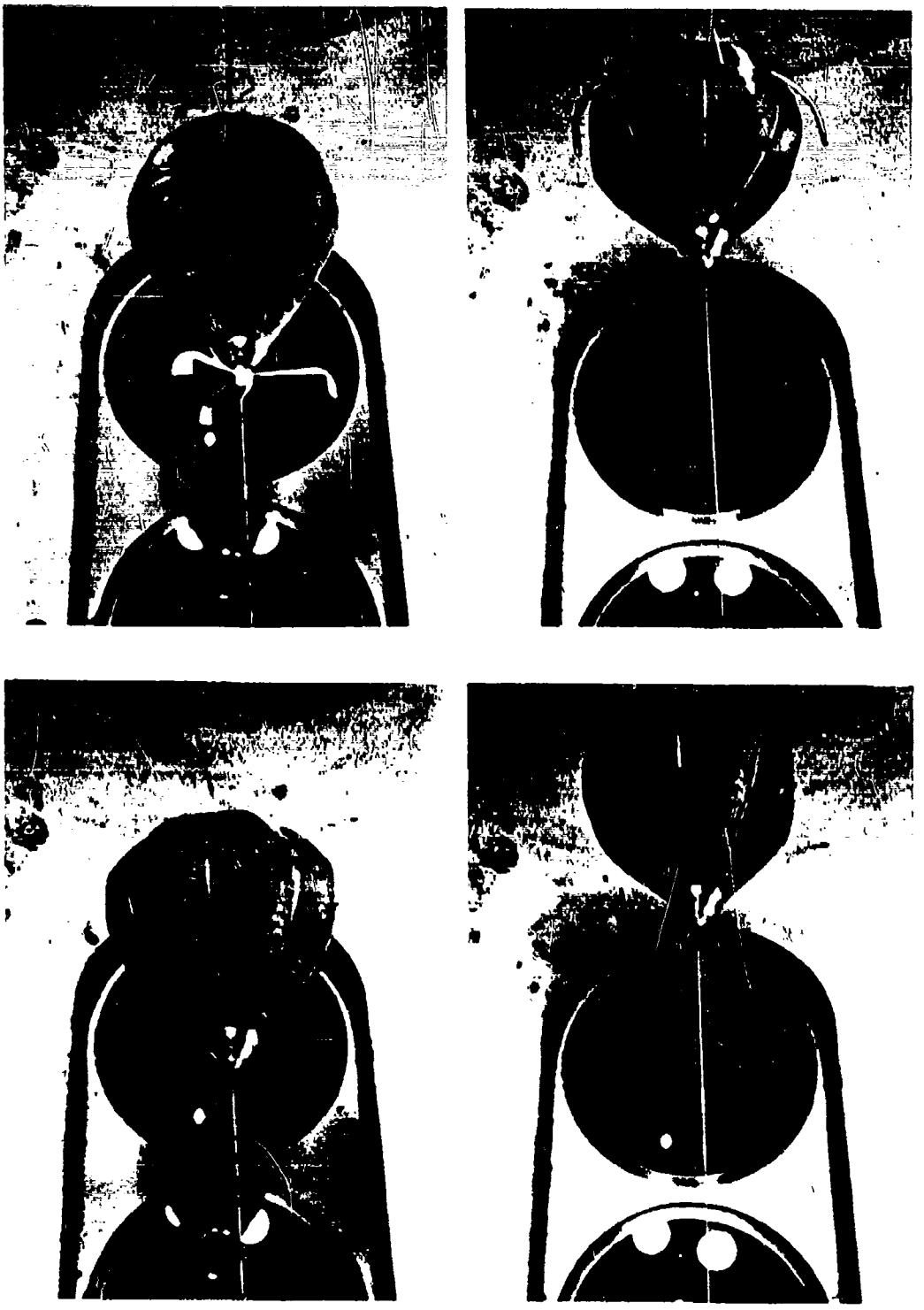

Fig. 5 Photographs of Flexible Models in the Tunnel at Mach 10

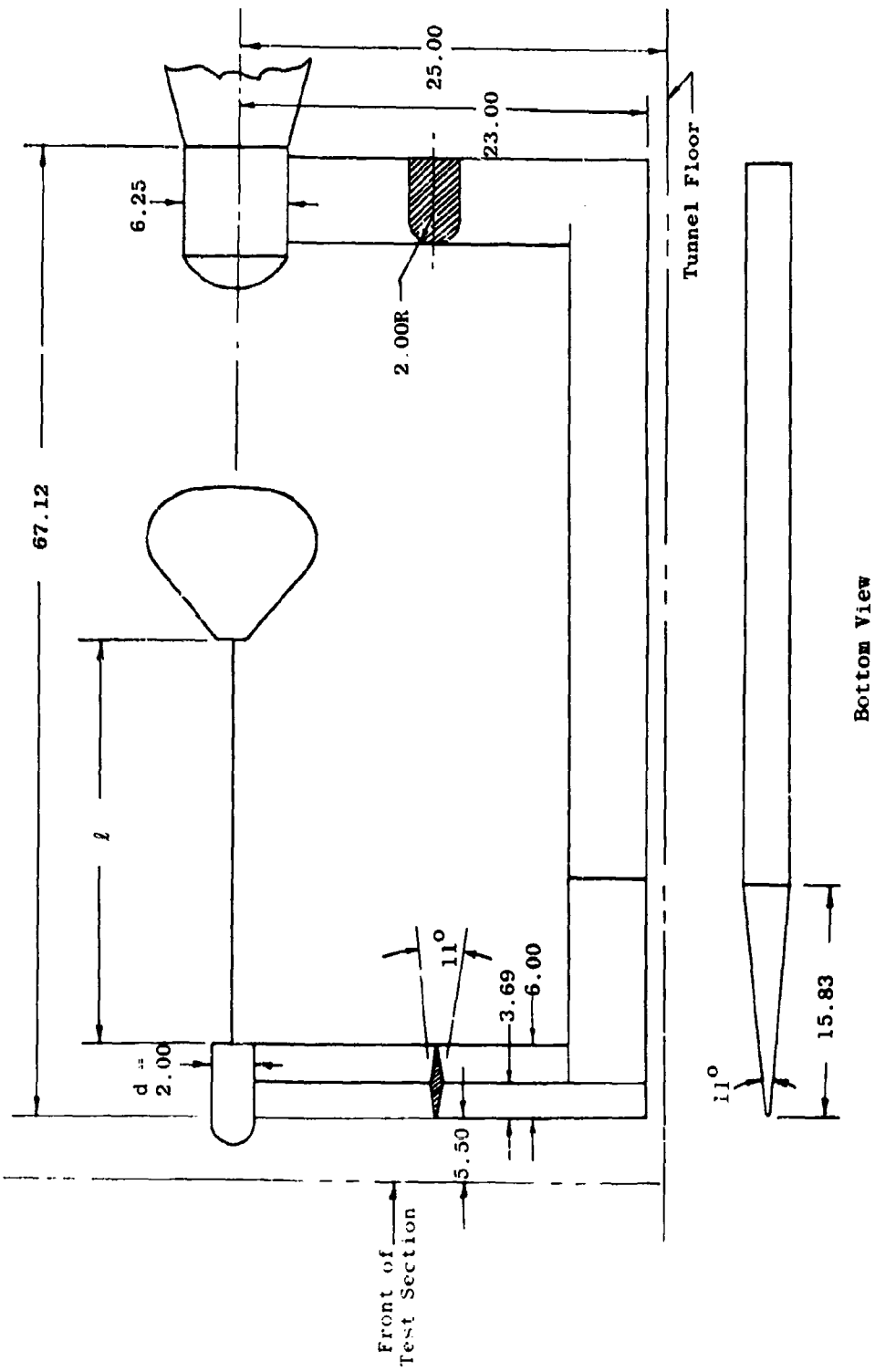

Fig. 6 Model Support Assembly for the Flexible Models

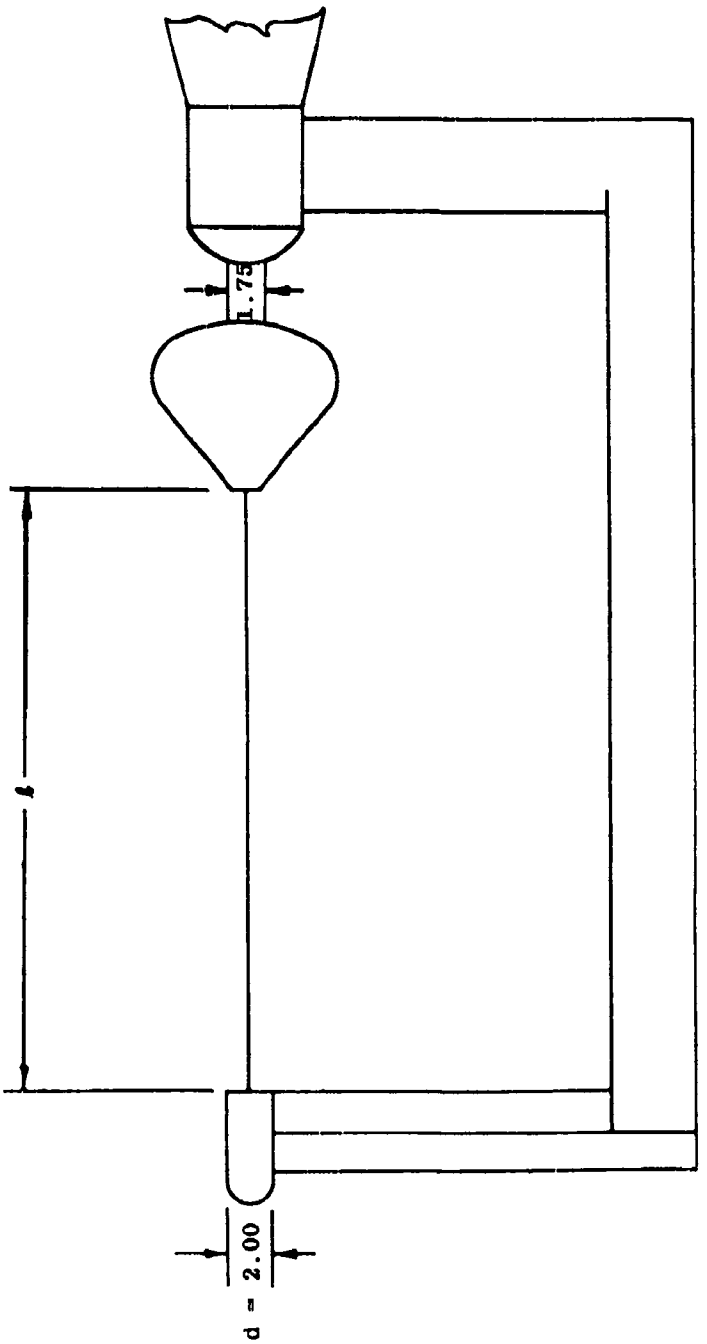

Fig. 7 Model Support Assembly for the Pressure and Heat Transfer Models

Fig. 8 Photograph of Pressure Model in the Tunnel Installation Chamber Showing Steel Balls Spot-Welded on Forebody

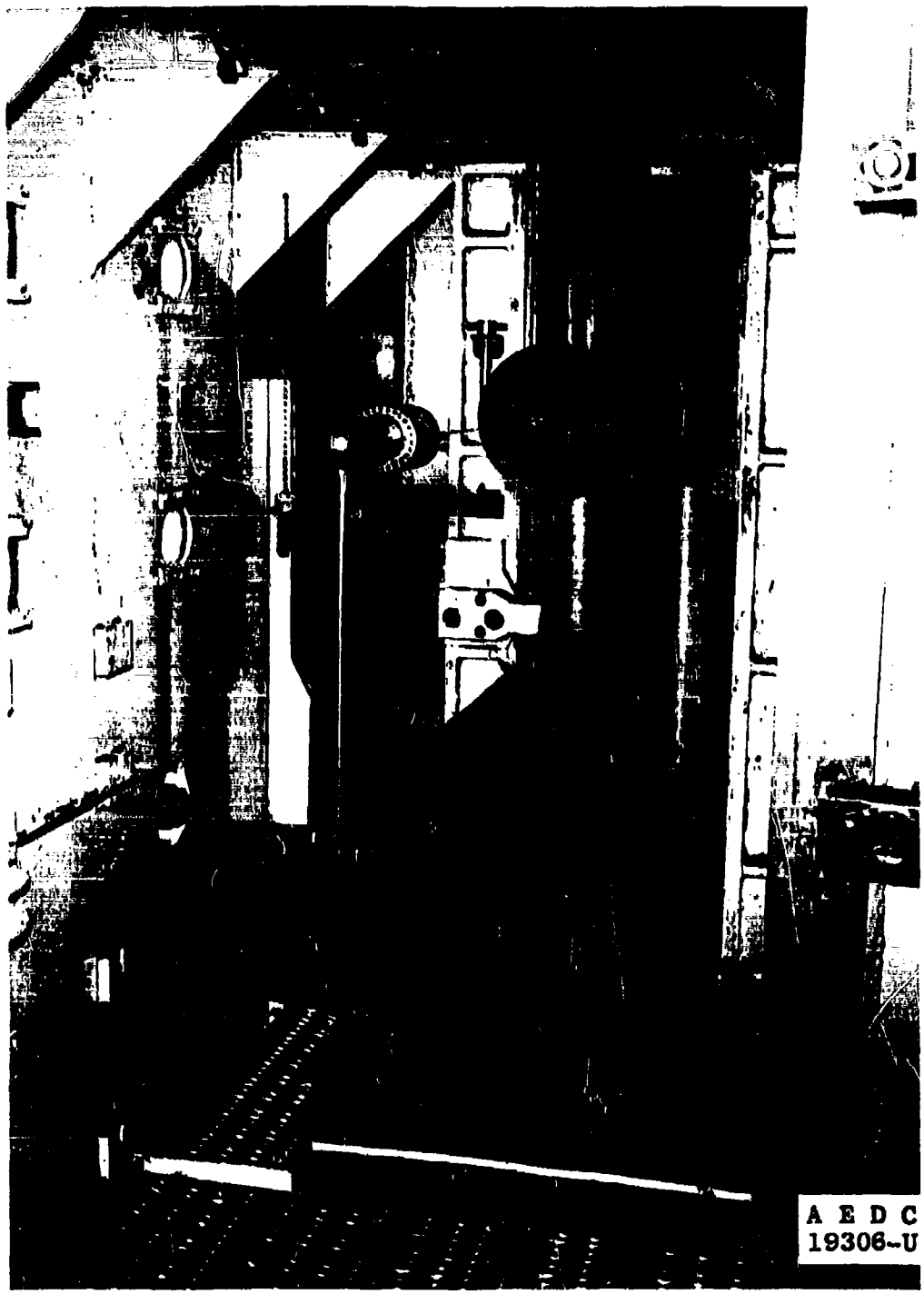

Fig. 9 Photograph of Pressure Model in the Tunnel Installation Chamber Showing Holes Drilled around Perimeter of the Cannister Step

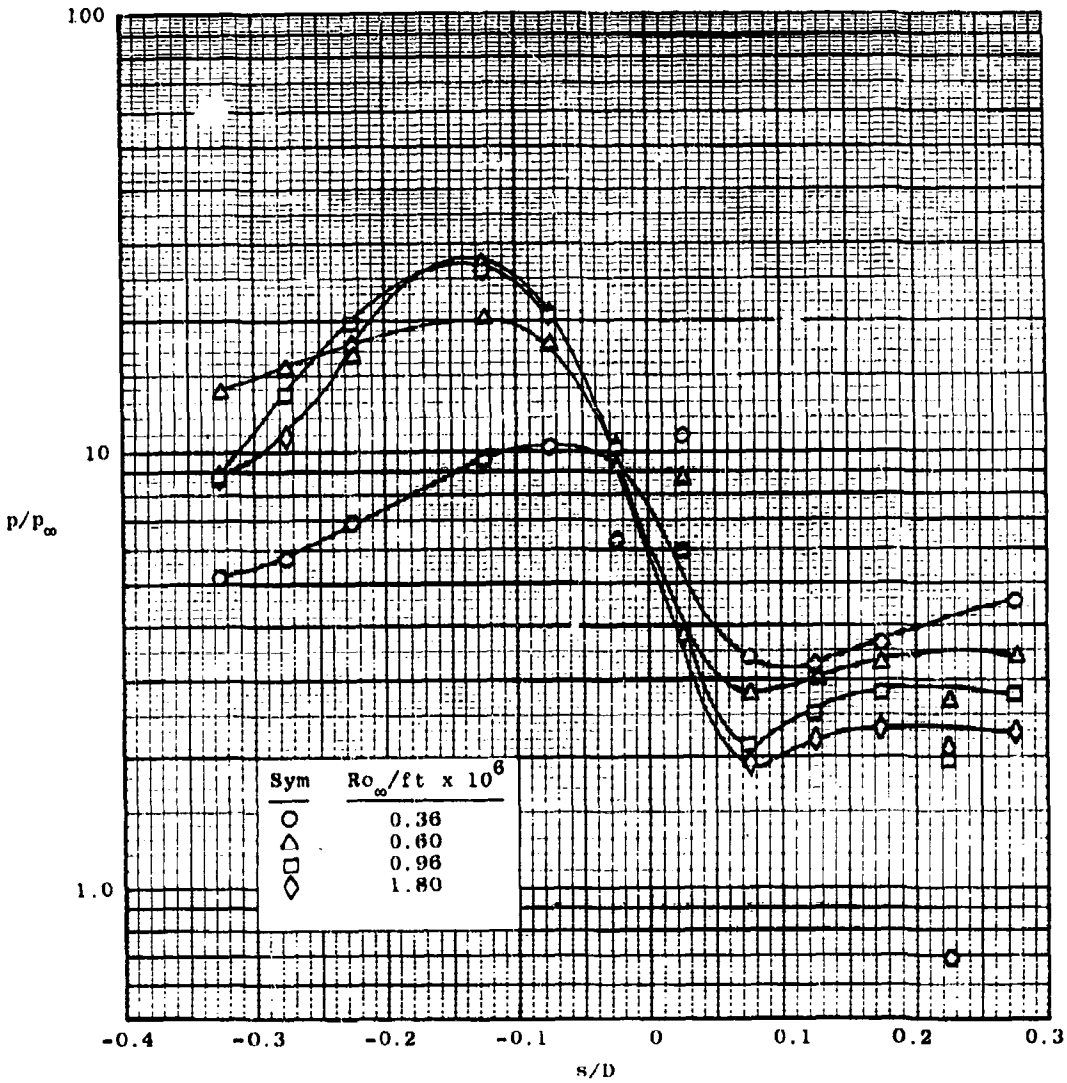

Fig. 10 Pressure Distribution Obtained behind the Forebody and Strut Assembly (Plugged Inlet)

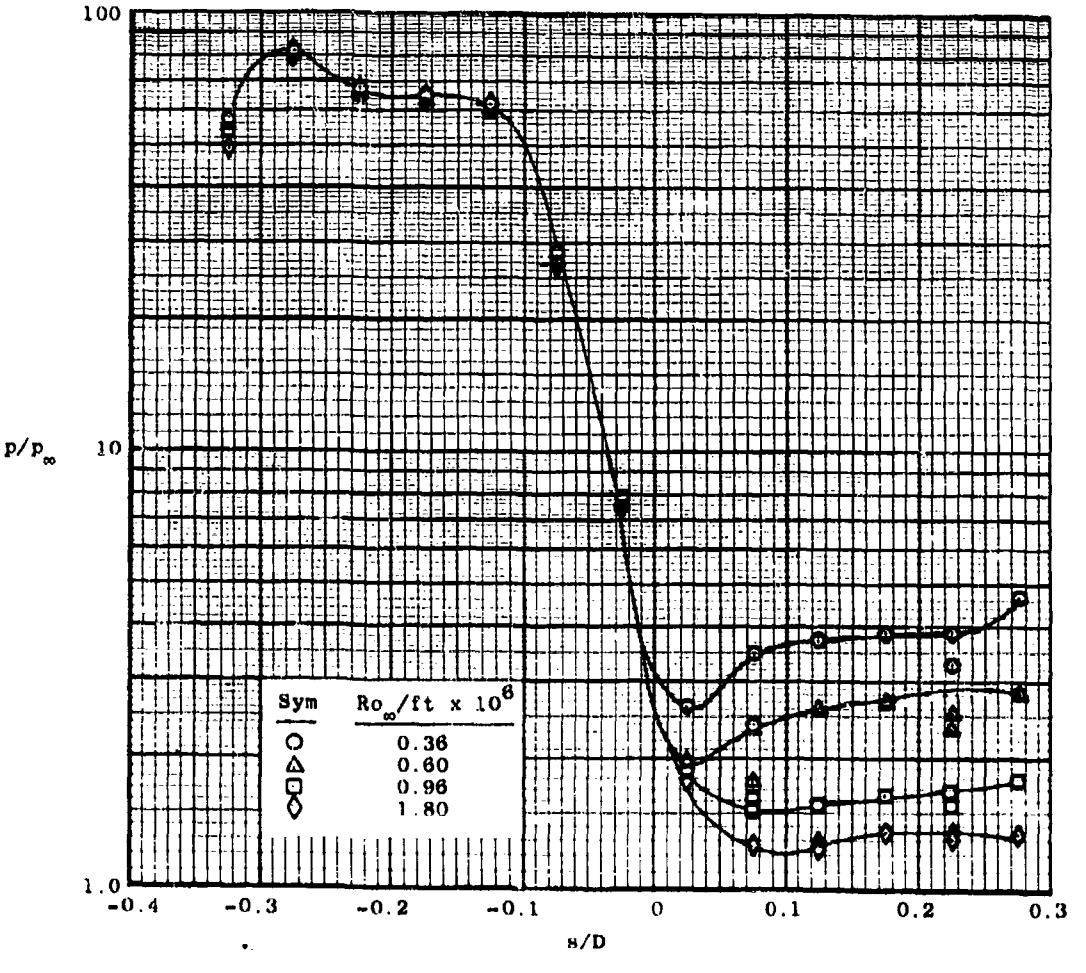

Fig. 11 Pressure Distribution Obtained without the Forebody and Strut Assembly (Plugged Inlet)

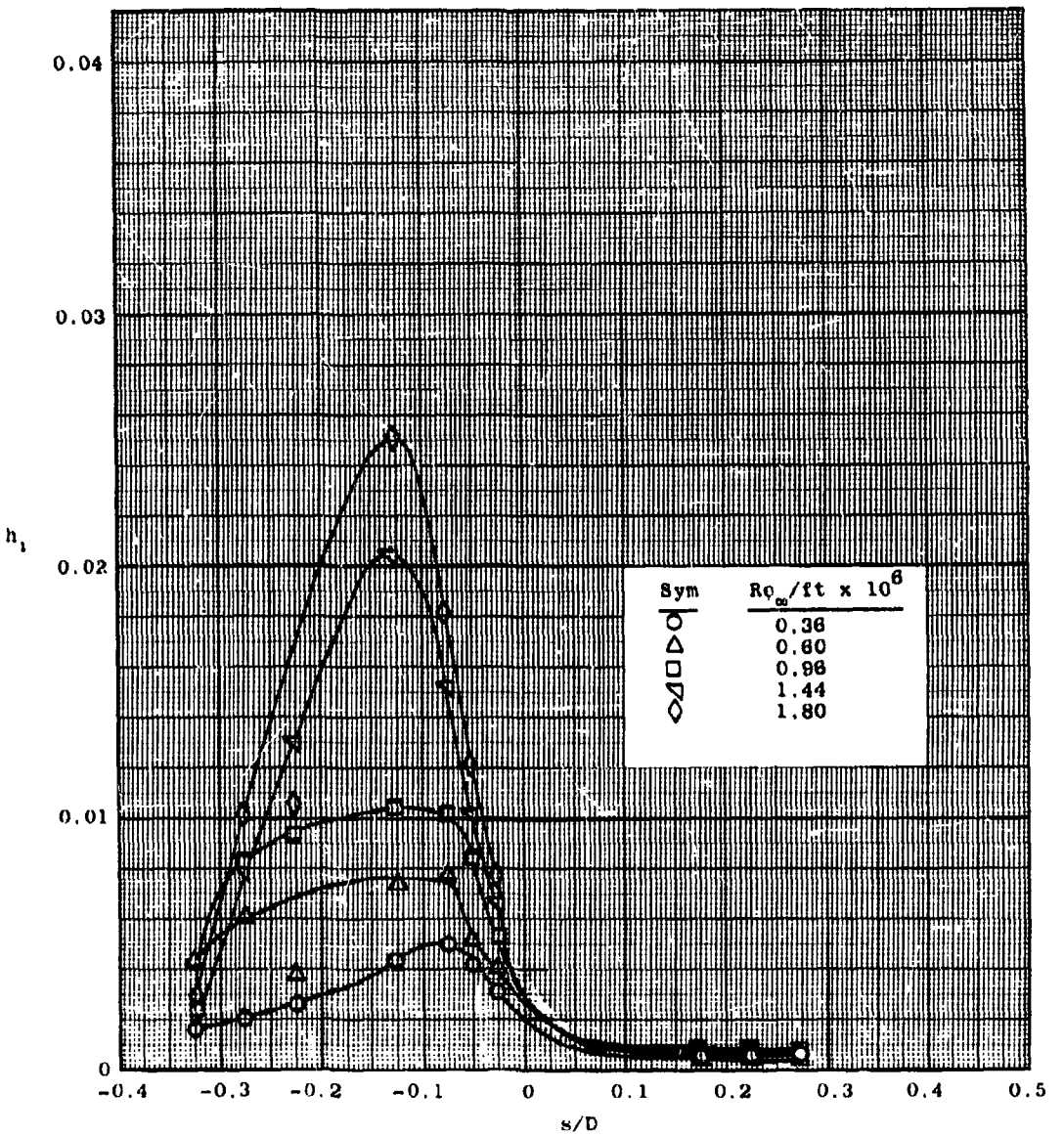

Fig. 12 Heat Transfer Coefficients on the Ballute When Mounted behind the Forebody and Strut Assembly (Plugged Inlet)

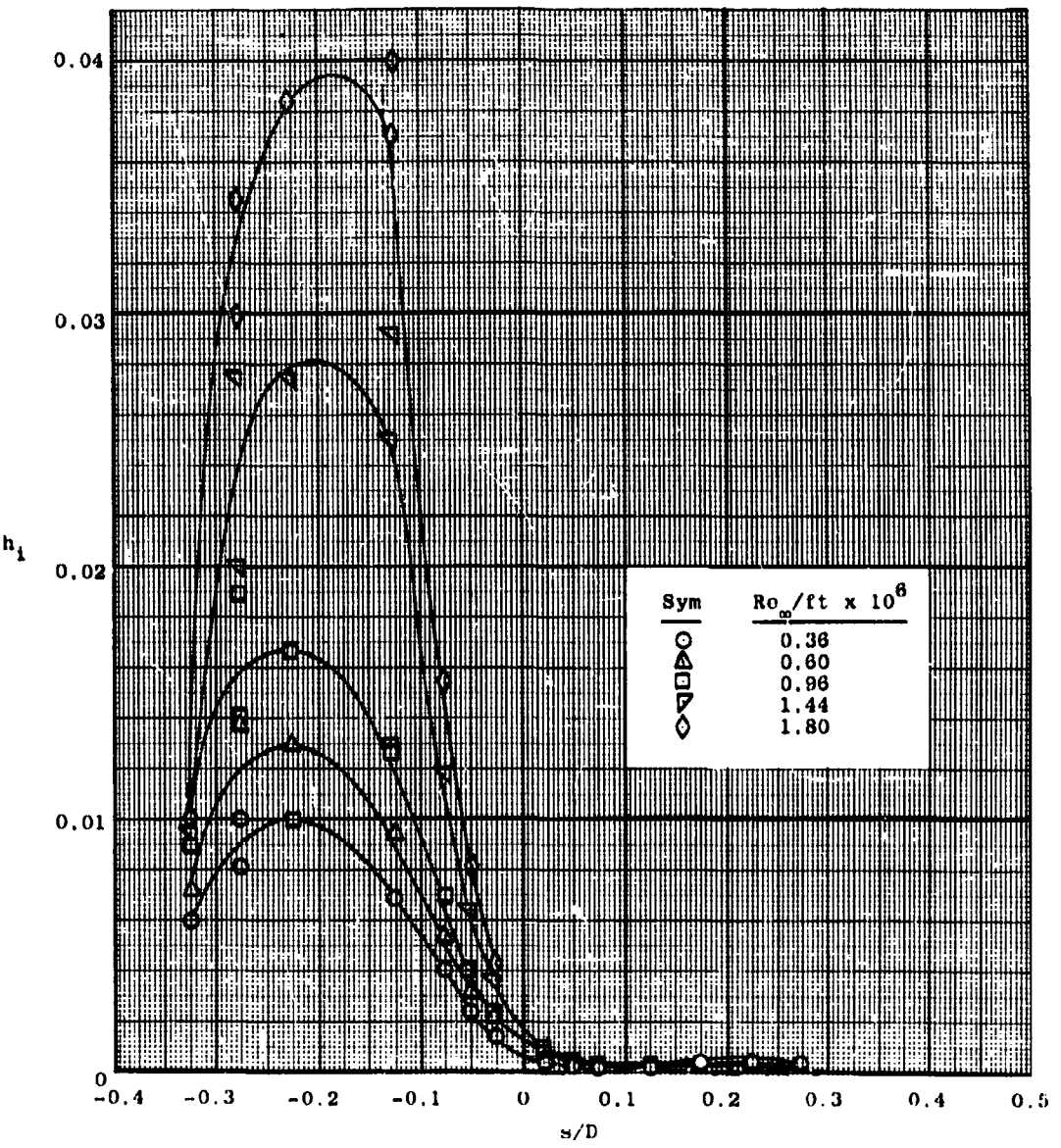

Fig. 13 Heat Transfer Coefficients Obtained without the Presence of the Forebody and Strut Assembly (Plugged Inlet)

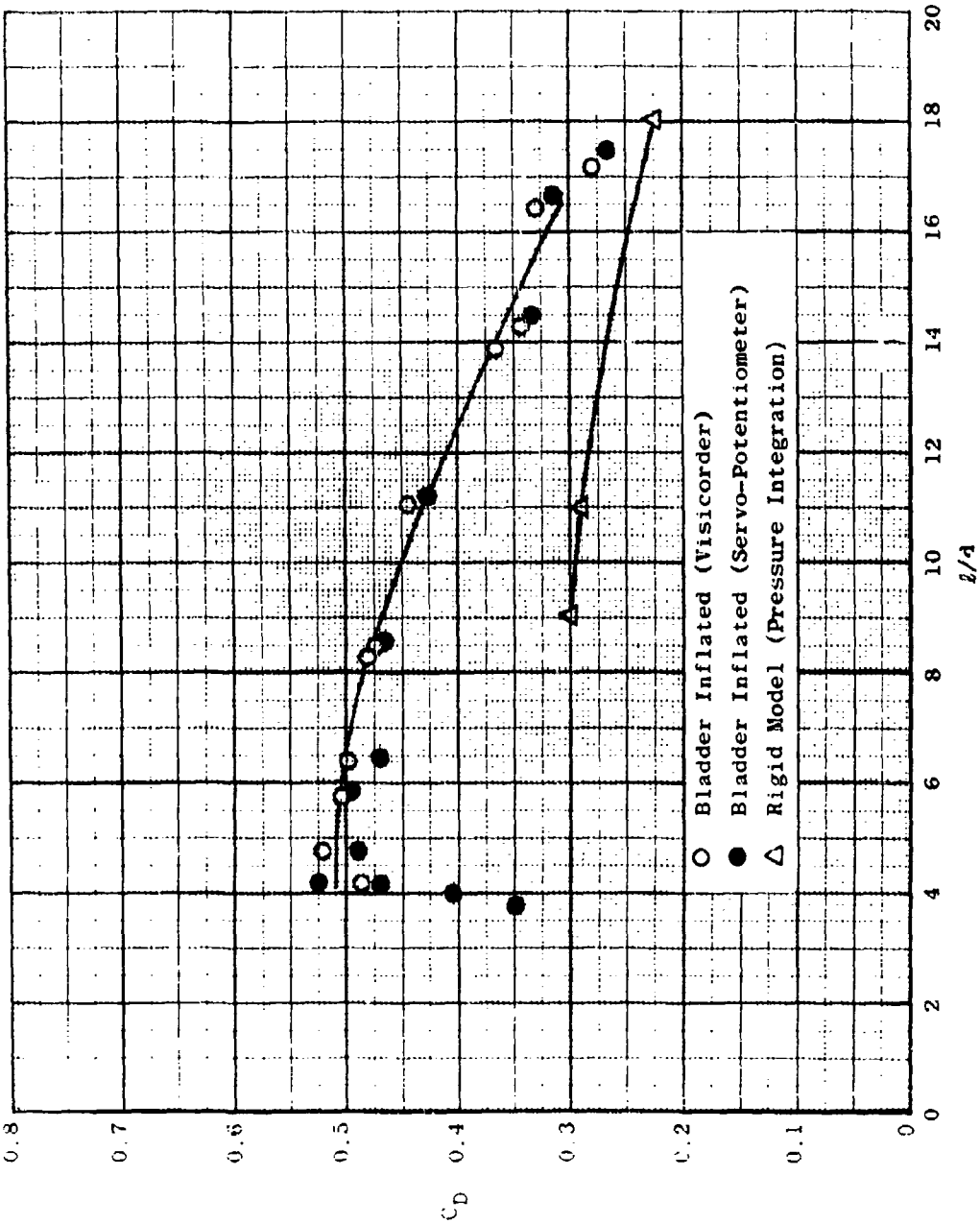

Fig. 14 Drag Coefficients on a Bladder Inflated Ballute and a Rigid Ballute, $Re_\infty/ft = 1.80 \times 10^6$

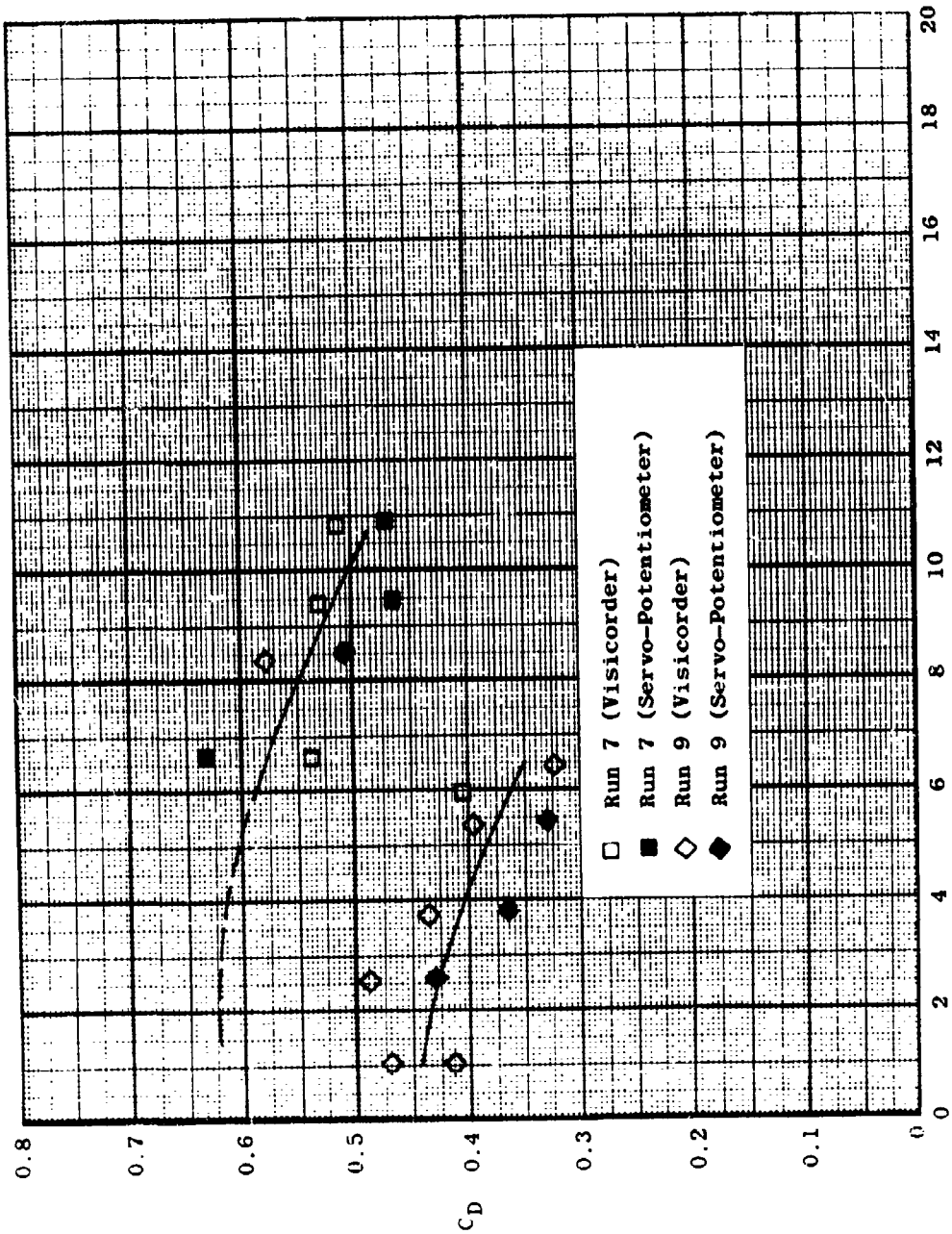

Fig. 15 Drag Coefficients on Flexible Models Inflated with Ram Air, $Re_\infty/ft = 0.96 \times 10^6$

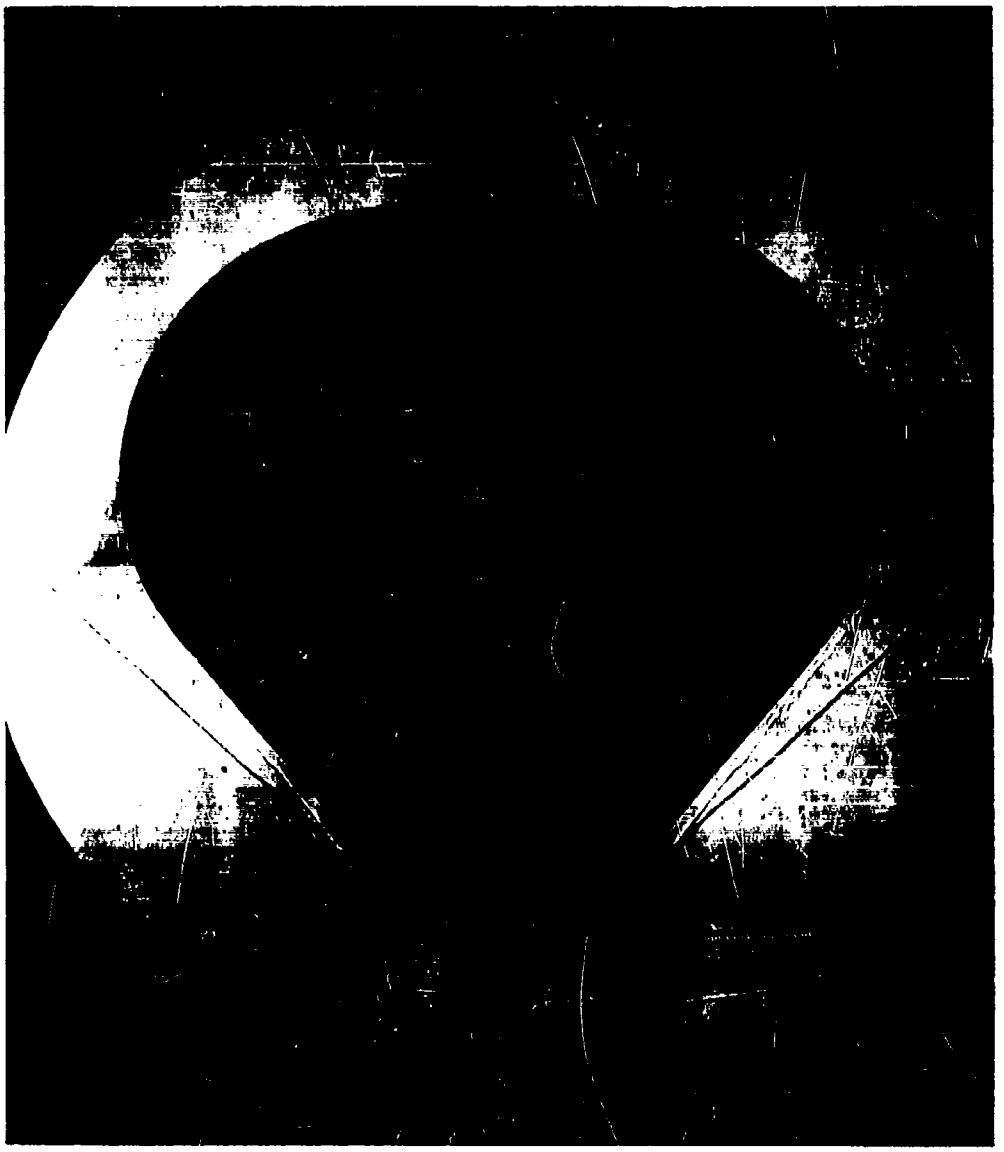

Fig. 16 Pressure Model Shadowgraph without Forebody and Strut; Plugged Inlet, $Re_\infty/ft = 1.80 \times 10^6$

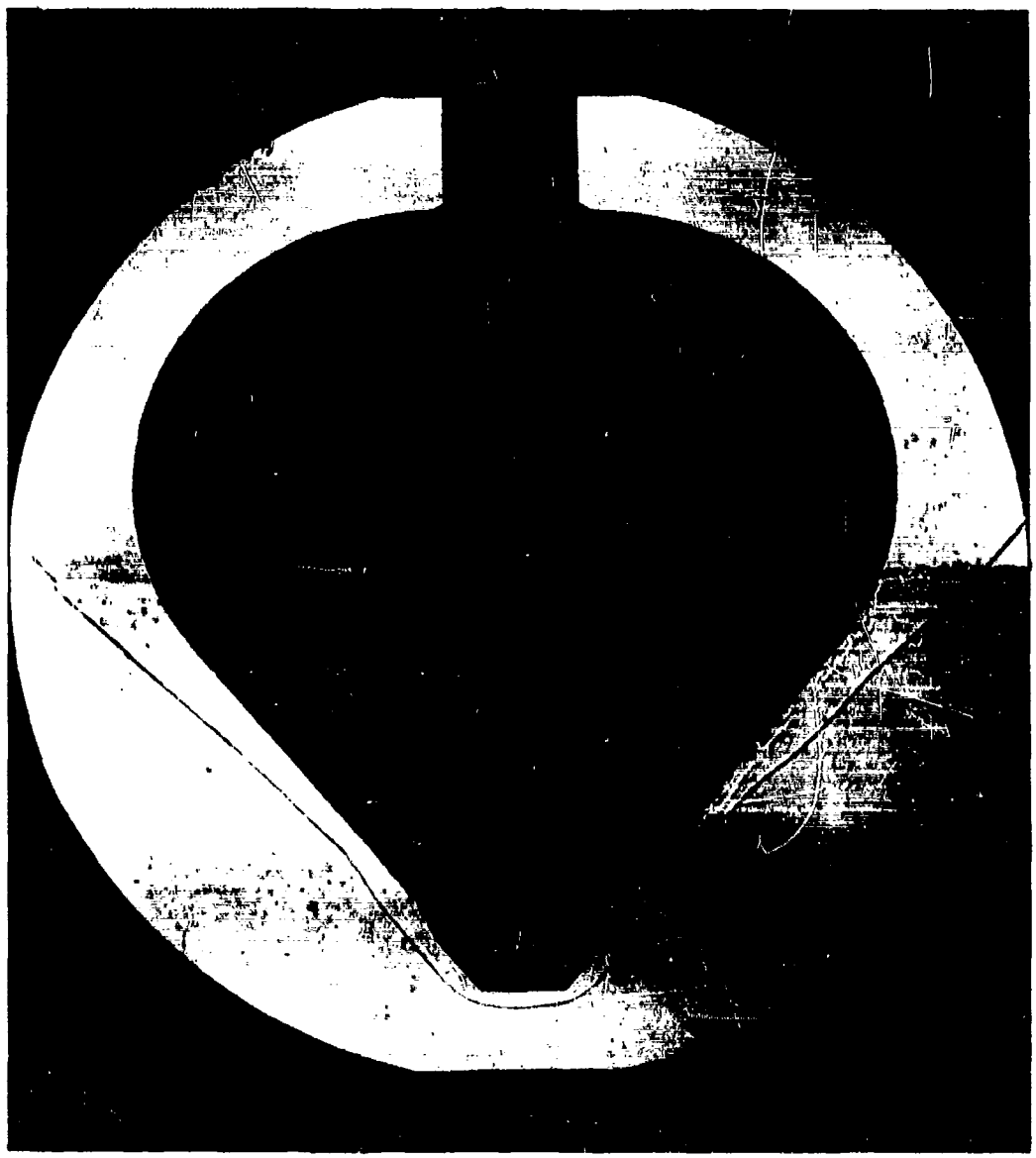

Fig. 17 Pressure Model Shadowgraph without Forebody and Strut; Open Inlet, $Re_\infty/ft = 1.80 \times 10^6$

Arnold Engineering Development Center
Arnold Air Force Station, Tennessee
Rpt. No. AEDC-TDR-62-39. PRESSURE DISTRIBUTION, HEAT TRANSFER, AND DRAG TESTS ON THE GOODYEAR BALLUTE AT MACH 10. March 1962, 25 p. incl 3 refs., illus.

Unclassified Report

Heat transfer and pressure distribution tests were conducted on rigid models of the ballute, and drag measurements were obtained on flexible models which were either inflated with ram air or pre-inflated with a bladder. The flexible models were fabricated from a woven stainless-steel cloth (Rene' 41 cloth) and impregnated with a silicone polymer to decrease porosity. The Reynolds number range investigated was from 0.36×10^6 to 1.80×10^6 per foot, and all data were obtained at zero angle of attack.

1. Balloons
2. Hypersonics
3. Recovery
4. Pressure
5. Heat transfer
6. Drag

I. AFSC Program Area 720F, Project 6065, Task 61256
II. Contract AF 40(600)-800 S/A 24(61-73)
III. ARO, Inc., AF Sta, Tenn.
IV. Kayser, L. D.
V. In ASTIA collection

Arnold Engineering Development Center
Arnold Air Force Station, Tennessee
Rpt. No. AEDC-TDR-62-39. PRESSURE DISTRIBUTION, HEAT TRANSFER, AND DRAG TESTS ON THE GOODYEAR BALLUTE AT MACH 10. March 1962, 25 p. incl 3 refs., illus.

Unclassified Report

Heat transfer and pressure distribution tests were conducted on rigid models of the ballute, and drag measurements were obtained on flexible models which were either inflated with ram air or pre-inflated with a bladder. The flexible models were fabricated from a woven stainless-steel cloth (Rene' 41 cloth) and impregnated with a silicone polymer to decrease porosity. The Reynolds number range investigated was from 0.36×10^6 to 1.80×10^6 per foot, and all data were obtained at zero angle of attack.

1. Balloons
2. Hypersonics
3. Recovery
4. Pressure
5. Heat transfer
6. Drag

I. AFSC Program Area 720F, Project 6065, Task 61256
II. Contract AF 40(600)-800 S/A 24(61-73)
III. ARO, Inc., AF Sta, Tenn.
IV. Kayser, L. D.
V. In ASTIA collection